SUMO1 Haploinsufficiency Leads to Cleft Lip and Palate

Fowzan S. Alkuraya,[1]* Irfan Saadi,[1]* Jennifer J. Lund,[1] Annick Turbe-Doan,[1] Cynthia C. Morton,[2] Richard L. Maas[1]†

Cleft lip with or without cleft palate (CL/P) is among the most common craniofacial birth defects. Several genes have been identified that contribute to CL/P, but the full spectrum of such genes and whether and how they interact is unknown. We identified a 5-year-old Caucasian girl born with unilateral cleft lip and palate (primary and secondary), who was otherwise phenotypically normal. Her karyotype was 46,XX,t(2;8)(q33.1;q24.3), and array CGH (comparative genomic hybridization) analysis was normal. Because the patient carried a balanced reciprocal translocation, we hypothesized that a gene important for palatogenesis was disrupted by the translocation. FISH (fluorescent in situ hybridization) analysis and suppression PCR (polymerase chain reaction) revealed that the *SUMO1* (small ubiquitin-related modifier) gene was interrupted by the 2q breakpoint, and *SUMO1* haploinsufficiency was further confirmed at the RNA and protein levels (Fig. 1A and fig. S1).

SUMO1 encodes a 101-residue polypeptide involved in posttranslational modification of many proteins (*1*). To establish a causative role for *SUMO1* haploinsufficiency in the pathogenesis of CL/P, we first examined the expression of murine *Sumo1* by whole-mount in situ hybridization at embryonic day 13.5 (E13.5) and observed strong expression in the upper lip, primary palate, and medial edge epithelia of the secondary palate (fig. S2). At E14.5, expression of *Sumo1* could be seen in the medial edge epithelial seam by using section in situ hybridization (fig. S2).

Next, we used an existing embryonic stem cell line in which *Sumo1* transcripts were interrupted by insertion of a β-*galactosidase*–expressing gene-trap vector into the *Sumo1* locus to generate $Sumo1^{Gt(pGT1Lxf)Byg}$ (henceforth referred to as $Sumo1^{Gt}$) mouse mutants. Wild-type transcripts were reduced in both hetero- and homozygotes, and variable reduction of Sumo1 protein was seen in heterozygotes. However, by X-gal staining, we detected that this hypomorphic allele faithfully recapitulated endogenous *Sumo1* expression in palatal shelf epithelium and mesenchyme at E13.5 (Fig. 1B). Several other genes required for palatogenesis, including *Eya1* (*2*) and *Msx1* (*3*), are expressed in palatal epithelium and/or mesenchyme at this time.

Among $Sumo1^{Gt/+}$ pups and embryos, 4 out of 46 (8.7%) exhibited cleft palate (Fig. 1C) or oblique facial cleft, compared with none in wild type (n > 100). In addition, the genotype distribution from heterozygous crosses at P1 (1:1.15:0.75) deviated from the expected 1:2:1. Both embryonic demise between E13.5 and E18.5 and immediate postnatal demise were noted (for *Sumo1* hetero- and homozygotes), indicating that *Sumo1* is required for other developmental functions besides palatogenesis.

Proteins encoded by three other genes, *MSX1*, *SATB2*, and *SMAD4*, are sumoylated and are either involved in or linked to pathways involved in palate morphogenesis (*4*–*7*). This suggests that *SUMO1* might control the activity of a repertoire of downstream effectors involved in palatogenesis, accounting for the sensitivity of palatal development to *SUMO1* gene dosage. To help place *SUMO1* in a molecular pathway relevant to its proposed role in CL/P, we tested for interaction between *SUMO1* and other cleft palate genes. Given its overlapping expression pattern with *Sumo1* in palatal shelf epithelium and mesenchyme, *Eya1* was an attractive candidate (fig. S2). Indeed, in $Sumo1^{Gt/+}$, $Eya1^{+/-}$ compound heterozygotes, the occurrence of cleft palate (36%) was significantly increased compared with that in $Sumo1^{Gt/+}$ (8.7%) (P < 0.037, Fisher exact test), or $Eya1^{+/-}$ (0%). Furthermore, we found Eya1 to be a substrate for sumoylation with SUMO1 in vivo. This was confirmed by abolishing the sumoylated Eya1 species with a SUMO-specific peptidase, SENP1. Furthermore, an Eya1 mutant protein in which two of three predicted high probability lysine residues were replaced with arginine displayed minimal sumoylation (Fig. 1D). These results identify a specific role for *SUMO1* in mammalian development and suggest that sumoylation regulates a network of genes that converge in palate development.

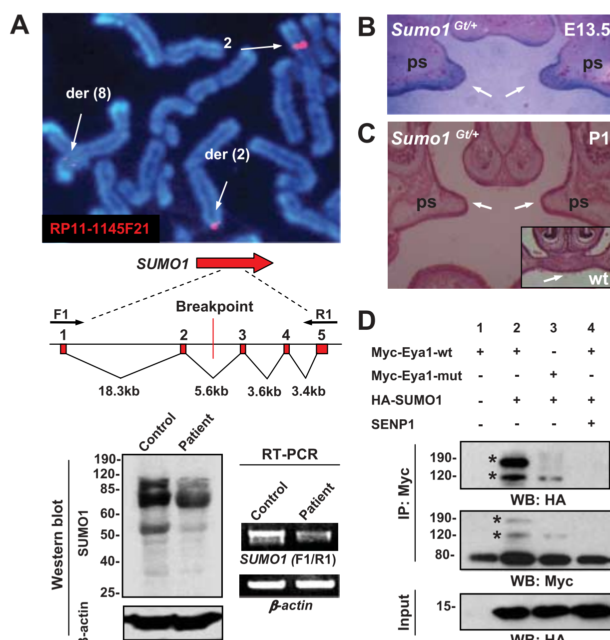

Fig. 1. (**A**) FISH using a clone that spans *SUMO1*. Location of the breakpoint is shown schematically. F1-R1 primers were used in reverse transcription PCR to show reduction of *SUMO1* expression in patient. Western blot shows reduced protein sumoylation in patient lymphoblasts compared with that of the control. (**B**) Coronal section of an E13.5 $Sumo1^{Gt/+}$ head showing *lacZ* expression in palatal shelf (ps) epithelium and mesenchyme. (**C**) Coronal section of a P1 $Sumo1^{Gt/+}$ head with ps elevated but not fused. (Inset) Normal control. (**D**) In the presence of hemagglutinin (HA)-tagged SUMO1, Myc-tagged Eya1 migrates as larger sumoylated species (*, lane 2), which disappear with the SUMO-specific peptidase, SENP1 (lane 4); the Eya1 $Lys^{43}\rightarrow Arg^{43}/Lys^{459}\rightarrow Arg^{459}$ (K43R/K459R) (Eya1-mut) shows markedly reduced sumoylation (lane 3).

References and Notes

1. G. Gill, *Curr. Opin. Genet. Dev.* **15**, 536 (2005).
2. P. X. Xu *et al.*, *Nat. Genet.* **23**, 113 (1999).
3. I. Satokata, R. Maas, *Nat. Genet.* **6**, 348 (1994).
4. D. R. FitzPatrick *et al.*, *Hum. Mol. Genet.* **12**, 2491 (2003).
5. G. Dobreva, J. Dambacher, R. Grosschedl, *Genes Dev.* **17**, 3048 (2003).
6. H. Lee *et al.*, *Genes Dev.* **20**, 784 (2006).
7. X. Lin *et al.*, *J. Biol. Chem.* **278**, 18714 (2003).
8. We thank G. Gill for generously providing expression vectors and members of the Developmental Genome Anatomy Project Consortium for their support. We also thank the patient, her family, and B. J. Negrini for their help and Unique for their assistance in recruitment. This work was supported by NIH grants GM061365 (C.C.M.), DE11697 and DE015246 (R.L.M.), and HD043430 to D. Beier (A.T.-D.), and a Canadian Institutes of Health Research postdoctoral fellowship (I.S.).

Supporting Online Material

www.sciencemag.org/cgi/content/full/313/5794/1751/DC1
Materials and Methods
Figs. S1 and S2
References

6 April 2006; accepted 18 July 2006
10.1126/science.1128406

[1]Division of Genetics, Department of Medicine, Brigham and Women's Hospital and Harvard Medical School, NRB-458, 77 Louis Pasteur, Boston, MA 02115, USA. [2]Department of Obstetrics and Gynecology and Reproductive Biology and Department of Pathology, Brigham and Women's Hospital and Harvard Medical School, NRB-160d, 77 Louis Pasteur, Boston, MA 02115, USA.

*These authors contributed equally to this work.
†To whom correspondence should be addressed. E-mail: maas@genetics.med.harvard.edu

Downloaded from www.sciencemag.org on August 25, 2008

www.sciencemag.org/cgi/content/full/313/5794/1751/DC1

Supporting Online Material for

SUMO1 Haploinsufficiency Leads to Cleft Lip and Palate

Fowzan S. Alkuraya, Irfan Saadi, Jennifer J. Lund, Annick Turbe-Doan, Cynthia C. Morton, Richard L. Maas*

*To whom correspondence should be addressed. E-mail: maas@genetics.med.harvard.edu

Published 22 September 2006, *Science* **313**, 1751 (2006)
DOI: 10.1126/science.1128406

This PDF file includes:

Materials and Methods
Figs. S1 and S2
References

Materials and Methods

Cytogenetics. Peripheral blood specimens were collected with informed consent. Cell transformation was performed using standard protocols (*S1*). The karyotype was at a resolution of 550 bands. CGH microarray analysis was performed using the Spectral Genomics 1Mb microarray chip. Cell suspensions from the cell lines were used in all the FISH experiments performed. The probes used were derived from BACs, PACs, or long-range PCR products. Probes mapping to the region of the cytogenetically determined breakpoints were selected from the UCSC Human Genome Browser (www.genome.ucsc.edu). Probe DNA was labeled by nick translation with Spectrum Green or Spectrum Red (Vysis), denatured and hybridized to chromosomal preparations fixed to microscope slides (*S2*). The ~50 kb breakpoint minimal region on der(8) was interrogated using 5 long-range PCR probes (10 kb each), one of which was found to span the breakpoint. Three PCR probes (4 kb each) were used to further narrow the breakpoint to a ~4 kb region that was analyzed using suppression PCR **(Fig. S1).**

Suppression PCR. Patient and control DNAs were digested with *Pvu*II and *Msc*I to create a restriction map of the der(8) ~4 kb minimal region. Subsequent ligation with adaptors and PCR was performed as described (*S3*). The resulting aberrant band was sequenced and this data was used to design primers across the der(2) breakpoint. Both breakpoints were cloned and sequenced **(Fig. S1).**

RT-PCR. RNA was extracted from patient lymphoblasts using the RNeasy Mini Kit (QIAGEN). RT-PCR was performed using the SuperScript one-step RTPCR Kit (Invitrogen). Primers are available upon request.

Generation of *Sumo1*$^{Gt(pGT1Lxf)Byg}$ mice. The BayGenomics gene-trap cell line

RRQ016 on a 129P2/OlaHsd background was selected for blastocyst injection. The resulting chimeras were bred to C57BL6/J females to obtain founder heterozygous mice *Sumo1*$^{Gt(pGT1Lxf)Byg}$ (henceforth referred to as *Sumo1*$^{Gt/+}$). These were subsequently mated to obtain 10 litters (58 pups) at P1 for phenotype analysis and used to generate the observed ratio (1.0 : 1.15 : 0.75) of wildtype (20): heterozygotes (23): homozygotes (15). Additional intercross experiments yielded 23 *Sumo1*$^{Gt/+}$ pups and 11 *Sumo1*$^{Gt/+}$, *Eya1*$^{+/-}$ compound heterozygotes. The Fisher exact test was used to compare the ratio of clefting in *Sumo1*$^{Gt/+}$ pups (4 out of 46) to that in *Sumo1*$^{Gt/+}$, *Eya1*$^{+/-}$ compound heterozygotes (4 out of 11). Genotyping of the *Sumo1*^{Gt} allele was performed using an upstream (rs13475883) and a downstream (rs3659238) SNP to *Sumo1* that distinguish the 129P2/OlaHsd (gene trap allele-containing) and C57BL6/J (wild type) backgrounds. *Eya1*$^{+/-}$ was genotyped as previously described (*2*).

Detection of *β-galactosidase* expression (X-gal staining). E13.5 heads were fixed (1% formaldehyde, 0.2% glutaraldehyde, 2 mM $MgCl_2$, 5 mM EGTA, 0.02% NP-40 in PBS) for 60 minutes at room temperature followed by staining (5 mM $K_3Fe(CN)_6$, 5 mM $K_4Fe(CN)_6$, 2 mM $MgCl_2$, 0.01% sodium deoxycholate, 0.02% NP-40, 1 mg/ml X-gal) for 90 minutes. Samples were post-fixed in 4% paraformaldehyde and processed for paraffin embedding. Sections were cut at 10 µm thickness and counter-stained with eosin to observe X-gal staining at the cellular level.

Histological procedures and in situ hybridization. For histological analysis, tissues were fixed in either 4% paraformaldehyde or in Bouin's solution, dehydrated in ethanol, and embedded in paraffin. Serial sections at 7 µm were stained with hematoxylin/eosin. Whole-mount in situ hybridization experiments were performed as previously described (*S4*). Reagents and probes are available upon request.

Site-directed mutagenesis. The QuikChange site-directed mutagenesis kit (Stratagene) was used to change the lysines at positions 43 and 459 of Myc-Eya1 to arginines (K43R, K459R). The amino acid residues are numbered according to *S4* The sequence of the primers used is available upon request.

Cell culture and coimmunoprecipitation assays. 293T cells were cultured in 75 cm^2 flasks under 5% CO_2. Approximately 1.5 x 10^6 293T cells were cultured in 100 mm dishes for 24 h and transfected with *Myc-Eya1*, *HA-SUMO1* and *UBC9* plasmid DNAs using 3 μl FuGENE6 (Roche) per 1 μg plasmid DNA following the manufacturer's instructions. 48 h following transfection, cells were initially lysed in 50 μl of SDS containing modified RIPA buffer (1% SDS, 20 mM Tris-HCl pH 8.0, 1% NP-40, 131 mM NaCl, 10% glycerol, 2 mM EDTA, protease inhibitor cocktail (Roche), 50 mM NEM). The lysate was then diluted 10x in the modified RIPA buffer without SDS and pre-cleared for 30 min. with protein A-agarose beads (Sigma) prior to incubation with α-Myc-agarose beads (Sigma). Following overnight incubation, beads were washed 3x with lysis buffer and resuspended in SDS sample buffer, boiled for 5 min, and loaded on 11% SDS-polyacrylamide gel for electrophoresis. Western blots were performed with an α-HA (Sigma) and c-Myc antibody (9E10, Sigma) to detect sumoylated and unsumoylated Myc-Eya1 proteins using ECL reagents (Pierce).

Supporting references:

1. S. H. Bernacki *et al.*, *J Mol Diagn* 5, 227 (2003).
2. J. H. M. Knoll, P. Lichter, in *Current protocols in human genetics* N. C. D. et.al, Ed. (John Wiley, New York, 1994), vol. 1.
3. P. D. Siebert, A. Chenchik, D. E. Kellogg, K. A. Lukyanov, S. A. Lukyanov, *Nucleic Acids Res* 23, 1087 (1995).
4. P. X. Xu, I. Woo, H. Her, D. R. Beier, R. L. Maas, *Development* 124, 219 (1997).

Figure Legends:

Fig. S1. (A) Combination of BAC clones and long range PCR amplicons were used to progressively narrow the breakpoint on derivative chromosome 8 to ~4 kb. **(B)** FISH using the clone that spans the 8q breakpoint. **(C)** Result of suppression PCR after digestion with *Pvu*II and adaptor ligation. The aberrant band corresponding to the introduction of a novel *Pvu*II site from 2q is denoted by *. **(D)** Sequence of the aberrant band across the 8q breakpoint; this sequence information was used to generate a PCR ampilicon across the 2q breakpoint, whose sequence is shown below.

Fig. S2. (A) and **(B)** Whole mount in situ hybridization at E13.5 using *Eya1* and *Sumo1* probes, respectively, with arrows and arrowheads indicating expression in palatal medial edge (MEE) and lips, respectively. **(C)** and **(D)** In situ hybridization with the same probes on cryosections with arrows indicating expression in MEE seam.

Fig. S1

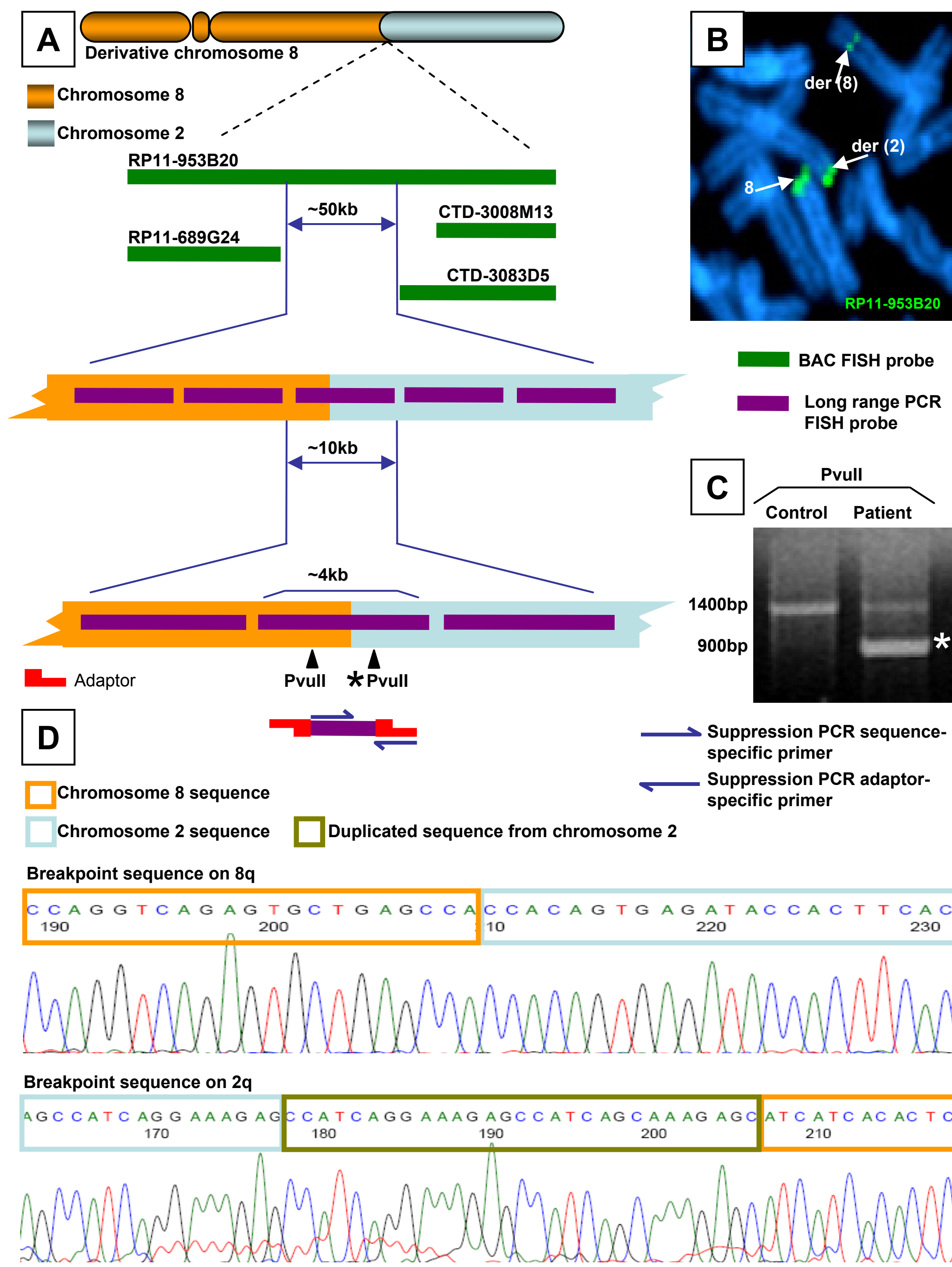

Fig. S2